Desalination and Water Treatment
www.deswater.com
doi: 10.1080/19443994.2014.947328

56 (2015) 709–721
October

Taylor & Francis
Taylor & Francis Group

Removal of congo red from aqueous solution by its sorption onto the metal organic framework MIL-100(Fe): equilibrium, kinetic and thermodynamic studies

S.E. Moradi[a], S. Dadfarnia[a,*], A.M. Haji Shabani[a], S. Emami[b]

[a]*Faculty of Science, Department of Chemistry, Yazd University, Yazd 89195-741, Iran, Tel. +98 351 8122667; Fax: +98 351 8210644; email: sdadfarnia@yazd.ac.ir (S. Dadfarnia)*
[b]*Faculty of Pharmacy, Department of Medicinal Chemistry and Pharmaceutical Sciences Research Center, Mazandaran University of Medical Sciences, Sari, Iran*

Received 26 March 2014; Accepted 21 June 2014

ABSTRACT

In this study, an iron based metal organic framework (MIL-100(Fe)) with high surface area and large pore volume has been synthesized by the hydrothermal method and its capability as an efficient sorbent for congo red (CR) removal from aqueous samples has been evaluated. The metal organic framework sorbent was characterized by Fourier transform infrared spectroscopy, scanning tunneling microscopy, thermogravimetric analysis/differential thermal analysis, and X-ray diffraction methods. The sorption capacity of the sorbent for CR was maximized through systematic studies of different factors which affect its sorption, such as contact time, initial concentration, sorbent dosage, pH and temperature. Sorption kinetic was studied in detail by four kinetic models, the pseudo-first-order and second-order equations, the Elovich equation and the intraparticle diffusion equation. The results indicate that the mechanism of the sorption process followed Elovich and pseudo-second-order kinetic. Sorption equilibrium was also studied with Langmuir, Temkin and Freundlich isotherm models. The sorption process followed Langmuir isotherm and the maximum monolayer sorption capacity for CR was found to be 714.3 mg g^{-1} of MIL-100(Fe).

Keywords: Metal organic framework; Langmuir isotherm; Congo red removal; Dye removal

1. Introduction

Dyes are the main contaminants of wastewater in many industries including textile, dyestuff, cosmetics, food coloring, papermaking, etc. [1]. Numerous dyes are available commercially and millions of tons of dyes are manufactured every year [2]. It has been estimated that annually 2% of the produced dyes is discharged in the effluent from manufacturing operations, and 10% is discharged from textile and the related products [3]. Thus, removal of dyes from water resources is very important because a slight amount of dye is highly visible; it controls the water quality and may disturb the aquatic life and the food web. Dyes can also cause allergic dermatitis and skin impatience. Some of them have been reported to be cancer-causing and the risk of human health due to the either toxic or mutagenic and carcinogenic effects [4–8].

*Corresponding author.

Congo red (CR) is the sodium salt of 3,3′-([1,1′-biphenyl]-4,4′-diyl)bis(4-aminonaphthalene-1-sulfonic acid) (the molecular structure of CR has been shown in Fig. 1). It is a secondary di-azo anionic dye, which is soluble in water. CR is used widely in textile, paper, painting, leather industries, etc. [9]. During the dyeing process, about 15% of the CR is released into the wastewaters and because of its intense color, it reduces the transmission of the sunlight into water which affects the aquatic plants and disturbs their ecosystem [10]. CR is very persistence in the natural environment and is metabolized to benzidine, a known human carcinogen. Furthermore, CR is considered as a mutagen and reproductive effector. It may also affect blood factors such as clotting and induce respiratory problems [10,11]. Thus, due to its toxicity and environmental effects, its removal from the wastewater samples is very important. Various methods including physical [11–21], chemical [22,23], and biodegradation [24] have been used for the dye removal. Among these methods, physical sorption is considered as the most attractive option due to its simplicity, high efficiency, and ease of operation. Different sorbents such as hen feathers [11] activated carbon [25], chitosan hydrogel [26], clay materials [27] and nanoparticles [28] have been used for the removal of CR.

Among the different sorbents used, the metal organic frameworks (MOFs) have attracted more attention for the removal of the organic and inorganic contaminants in water [29–31] due to their high physical and chemical stability, tunable pore size, functionalizable pore walls and large specific surface area [32–35]. Synthesis of MOFs was first reported by Yaghi in 1998 [36]. MOFs are crystalline materials, which are basically composed of a metal ion or a cluster of metal ions and an organic molecule called linker. MOFs have been applied in the sorption/storage of carbon dioxide [37,38] sorption of organic hazardous vapors [39], hydrogen storage [40] luminescence [41] and separation of chemicals [42]. MOFs have also been used in removal of some dyes including xylenol orange [43], methyl orange [44], and methylene blue [44,45].

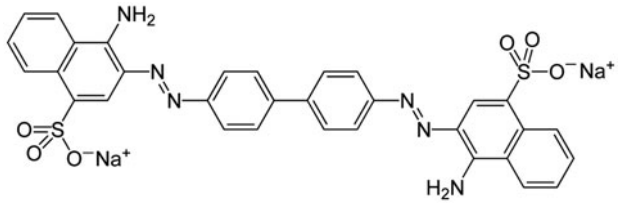

Fig. 1. Molecular structure of CR.

In the present work, an iron based microporous MOF sorbent (MIL-100(Fe)) with high surface area has been synthesized and characterized. Then, its capability in the removal of CR dye from the aqueous solution is considered and the parameters affecting the sorption including initial concentration of dye, temperature, pH, amount of sorbent and contact time are studied. Furthermore, sorption kinetic is studied in detail by four kinetic models, the pseudo-first-order and second-order equations, the Elovich equation and the intraparticle diffusion equation. Finally, the equilibrium behavior of the system is considered by Langmuir, Temkin and Freundlich isotherm models. The maximum monolayer sorption capacity of the sorbent for CR is also determined.

2. Experimental section

2.1. Materials

The reactants used in this study for the synthesis of the MOF sorbent (MIL-100(Fe)) were $FeCl_3{\cdot}6H_2O$ (99 wt%, Merck, Germany) as the metal source, trimethyl 1,3,5-benzenetricarboxylate (99 wt%, Merck, Germany) as the organic linker and doubly distilled water as the solvent.

CR ($C_{32}H_{22}N_6Na_2O_6S_2$, MW = 696.665) was purchased from Sigma–Aldrich, USA (98% purity). A stock solution of 1,000 mg L^{-1} of CR was prepared in double distilled water and the experimental solutions of the desired concentration were obtained through successive dilutions.

2.2. Preparation of MIL-100(Fe) sorbent

The MIL-100(Fe) was prepared according to the procedure reported by Canioni et al. [46] i.e. a mixture of $FeCl_3{\cdot}6H_2O$ (1.622 g) and trimethyl 1,3,5-benzenetricarboxylate (1.387 g) was dispersed into 50 mL of water and was heated for three days at 130°C in a Teflon lined autoclave. Then, the orange solid was recovered by filtration, washed with acetone and air dried. It was stored in a closed container and was used as the sorbent in further work.

2.3. Textural and structural studies

The porous structure of the surface modified samples was estimated by powder XRD (Philips 1830 diffractometer) using graphite monochromated CuKa radiation. STM images were obtained in the air by using Nano system Pars instrument (SS-1), Iran. In constant current mode using Pt/Ir tips at a positive sample bias of 100 mV and tunneling current of 0.1 nA.

The tips were previously tested on an highly ordered pyrolytic graphite standard sample to verify their suitability for topographic performances. Thermal analysis was carried out using STA503, Bähr (Thermoanalyse GmbH, Hüllhorst Germany). The instrument settings were at a heating rate of 10°C min^{-1} and an air atmosphere with 100 mL min^{-1} flow rate. Fourier transform infrared (FT-IR) spectrum of the sorbent was recorded at 30°C FT-IR spectrometer in the wavenumber range of 400–4,000 cm^{-1} applying the KBr pellet technique on a DIGILAB FTS 7000 spectrometer (Varian, Cambridge, MA, USA) equipped with an attenuated total reflection cell.

2.4. Batch sorption procedure

Batch mode sorption studies were carried out by mixing 0.01 g of MIL-100(Fe) with 50 mL of dye solution (10–200 mg L^{-1}) at a pH of ~6. The mixture was continuously shaken on a shaking bath with a speed of 250 rpm at 30°C until the equilibrium was achieved (typically 6 h). After the sorption was completed, the mixture was centrifuged at 3,000 rpm for 3 min and the amount of CR remained in the solution was determined by measuring its absorbance with a UV–vis spectrophotometer (CE 2501, CECIL instruments, Cambridge, UK) at wavelength of 493 nm (λ_{max}). The amount of the dye sorbed on the sorbent was determined by the following equation:

$$q_e = \frac{(C_o - C_e)V}{W} \tag{1}$$

where q_e is the equilibrium sorption capacity of the CR sorbed on the unit mass of the sorbent (mg g^{-1}); C_o and C_e are the initial and final (equilibrium) concentrations of the CR in solution (mg L^{-1}); V is the volume of the solution (L) and W is the mass of the sorbent (g). Each experiment was done three times and the arithmetic average of the results was determined.

The sorption kinetics of the anionic dye on the microporous sorbent as a function of time was also carried out at an initial dye concentration of 100 mg L^{-1} at a pH of ~6. The most commonly used pseudo-first-order, pseudo-second-order, Elovich and intraparticle diffusion models were applied to the analysis of the experimental data.

2.5. Error analysis

The linear least-squares method was used to compare the best-fitting of kinetic models (pseudo-first-order, pseudo-second-order, Elovich and intraparticle diffusion) and the sorption isotherms (Langmuir, Temkin, and Freundlich). In order to approve the best-fit isotherms and kinetic models for the sorption method, it is necessary to examine the data-set using the Chi-square test combined with the values of the determined coefficient (R^2). For this purpose, the coefficient of the determination R^2 of each model was determined using the following equation:

$$R^2 = \frac{\sum (q_m - \overline{q_e})^2}{\sum (q_m - \overline{q_e})^2 + \sum (q_m - q_e)^2} \tag{2}$$

where q_e is the equilibrium sorption capacity from the experiment (mg g^{-1}), and q_m is the equilibrium capacity calculated according to the dynamic model (mg g^{-1}) and $\bar{q_e}$ is the average of q_e (mg g^{-1}).

The non-linear regression Chi-square (χ^2) test was employed as a criterion for the quality of fitting. The statistical analysis was based on the sum of the squares of the differences between the experimental sorption capacity and the data obtained from the models, with each squared difference divided by the corresponding data obtained by calculating the kinetic and thermodynamic models. The Chi-square was determined by the following equation:

$$\chi^2 = \sum \left[\frac{(q_e - q_m)^2}{q_m} \right] \tag{3}$$

where q_e is the equilibrium sorption capacity of the experiment (mg g^{-1}), and q_m is the equilibrium capacity calculated according to the dynamic model (mg g^{-1}). A large value of χ^2 shows that the data from the model is different from the experimental value, whereas, a small value of χ^2 indicates that the difference between them is insignificant.

3. Results and discussion

3.1. Textural characterization

The XRD pattern of MIL-100(Fe) (Fig. 2) shows high crystallinity with reflections in the 2θ range of 2°–12°. The closeness of the main peaks (2θ of 6.69° and 10.8°) to the reported values in literature confirms the right synthesis of the MIL-100(Fe) sorbent [46]. In order to understand the surface morphology, the shape and size of the iron based MOF, STM of the MIL-100(Fe) sorbent was recorded (Fig. 3). The 3D and 2D STM images (Fig. 3(a) and (b)) show that the MOF sorbent has a regular porous structure with a particle size of about 200 nm and the pores of 2 nm.

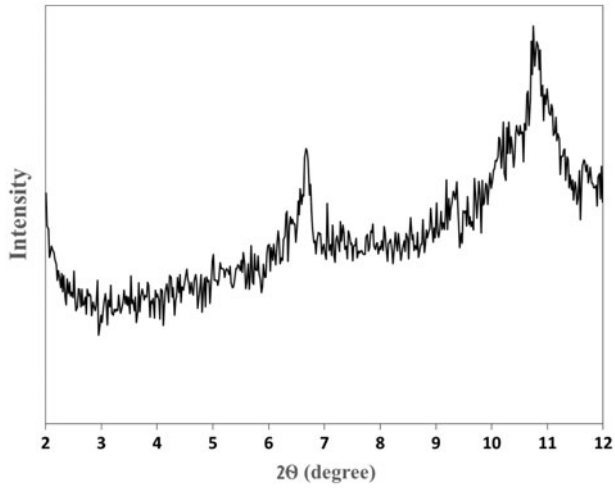

Fig. 2. Low angle XRD pattern of MIL-100(Fe) sample.

The thermogravimetric and differential thermal analysis curves of the MIL-100(Fe) (Fig. 4) indicated two weight losses within the 50–110˚C and 330–460˚C. The first weight loss is due to the departure of water, whereas the second weight loss is because of the removal of the solvent molecules and/or the decomposition of MIL-100(Fe) framework. This clearly indicates that the MIL-100(Fe) is thermally stable up to 330˚C.

The FT-IR spectrum of MIL-100(Fe) shown in Fig. 5(a) is similar to the previously reported spectrum [46,47]. In this spectrum, the band at 1,721 cm^{-1} corresponds to the C=O; the band at 3,085 cm^{-1} is owing to the C–H of the aromatic groups and the one at 1,381 and 1,452 cm^{-1} are due to O–C–O stretching. The bands at 934 and 1,109 cm^{-1} can be related to the vibrations of benzene rings [48]. Furthermore, the FT-IR spectra of CR (5b) and MIL-100(Fe) loaded with CR (5c) are also reported. The major differences in the spectra after the dye sorption are: the appearance of the band at 3,446 cm^{-1} (Fig. 5(c)) correspondent with the stretching vibration of –N–H in the structure of CR; the shift and the reduction of the bands at 3,085 cm^{-1} and 1,721, cm^{-1} of Fig. 5(c) in comparison with the Fig. 5(a) assigned to aromatic C–H and C=O stretching, respectively. This result indicated that the NH_2, N–N and $–SO_3$ groups of CR were involved in the sorption process. Furthermore, the bands at 1,550, 1,506, 1,400 cm^{-1} (Fig. 5(b)), attributed to aromatic structure vibrations, have been shifted, broadened, and reduced after the sorption which indicate that the CR on MIL-100(Fe) is held by chemical activation or chemisorption, probably indicating the CR and MIL-100(Fe) complexation.

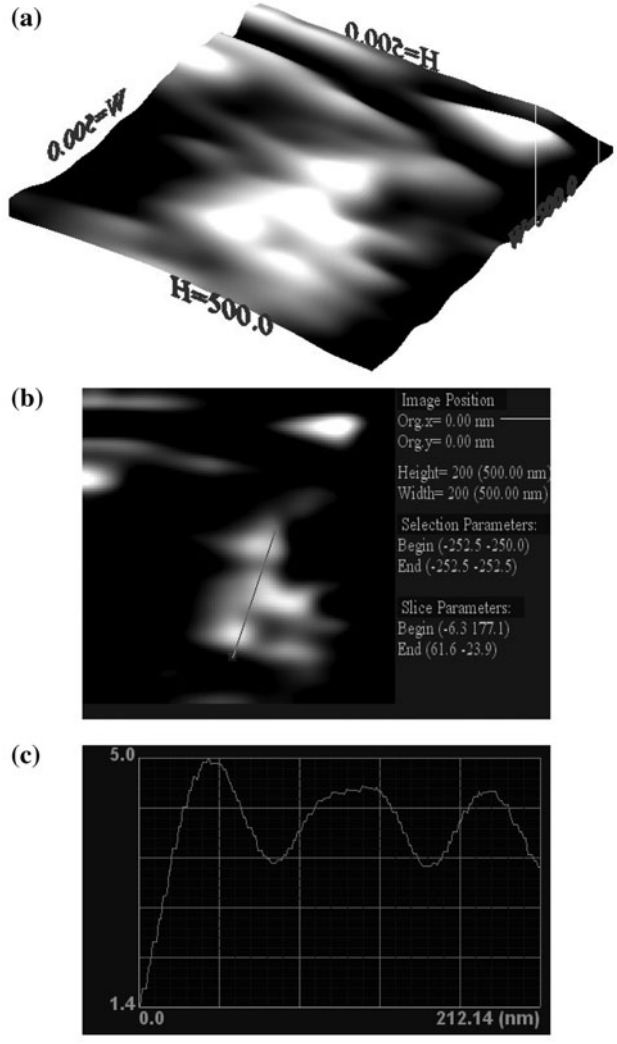

Fig. 3. STM micrographs of MIL-100(Fe) (a) 3D, (b) 2D, and (c) size marker.

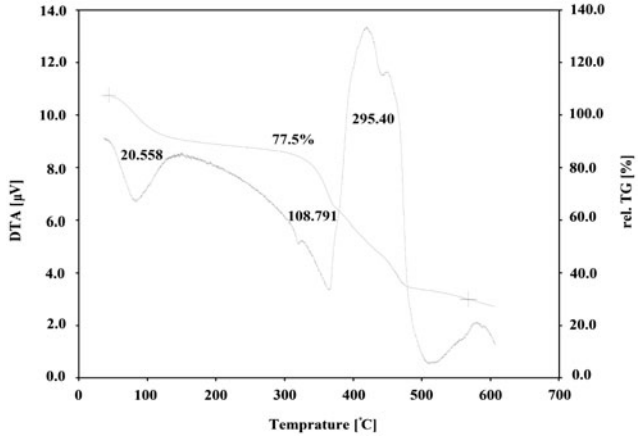

Fig. 4. DTA/TG images of MIL-100(Fe).

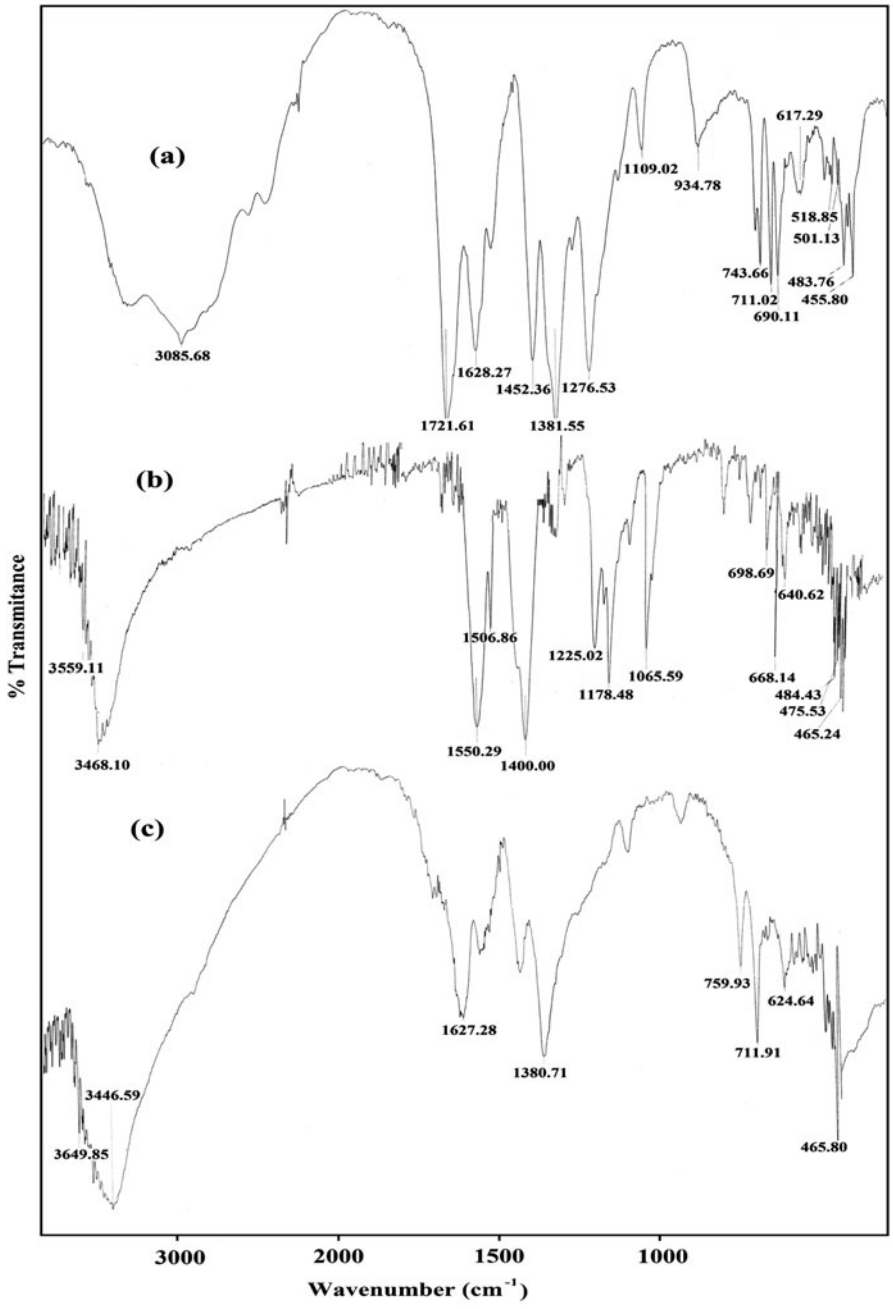

Fig. 5. FT-IR spectra of (a) MIL-100(Fe), (b) CR and (c) CR loaded MIL-100(Fe).

3.2. Sorption studies

3.2.1. Effect of contact time and initial concentration

The equilibration time and the kinetics of sorption process were studied by considering the sorption behavior of different initial concentrations of CR (50, 80, and 100 mg L^{-1}) on MIL-100(Fe) vs. contact time at 30°C and at a pH of ~6. As shown in Fig. 6, an increase in initial concentration enhances the interaction between the CR molecules and the surface of the MOF sorbents. The CR molecules have to encounter the boundary layer effect before diffusing from boundary film onto the sorbent surface followed by its diffusion into the porous structure of the sorbent which eventually takes relatively longer contact time. The time profile of the CR uptake by the sorbent is a single, smooth and continuous curve leading to a saturation point [49]. In addition, increasing the initial dye

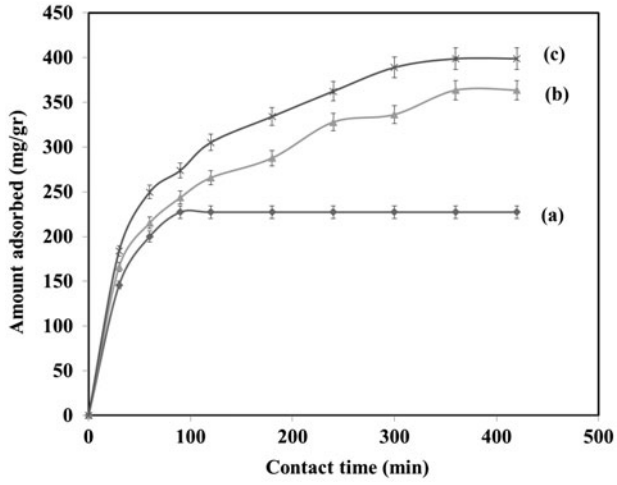

Fig. 6. Effect of initial concentration ((a) 50 mg L^{-1}, (b) 80 mg L^{-1} and (c) 100 mg L^{-1}) on removal of CR by MIL-100 (Fe), (agitation speed = 250 rpm, sorbent dosage = 0.2 g L^{-1}, temperature = 30˚C, pH 6).

concentration increases the amount of collisions between the CR molecules and the sorbent which improves the sorption procedure. Furthermore, Fig. 6(b) and (c) clearly indicates that the removal capacity increased quickly up to 2 h and then slowly up to 6 h where the sorption equilibrium was achieved. It should be noted that with an initial CR concentration of 50 mg L^{-1}, after 2 h the dye was completely removed from the solution.

3.2.2. Amount of sorbent

The effect of the amounts of MOF sorbent (0.02–0.5 g L^{-1}) on the removal of dye was studied. The experiments were carried out at an initial concentration of 80 mg L^{-1} of CR, 30˚C, pH of ~6 and the equilibration time of 6 h. It was found that the amount of dye remained in the solution was decreased with an increase in the amount of the MOF sorbent. Based on this observation, a capacity of 547 mg of dye per gram of sorbent equivalent to 0.1 g L^{-1} (sorbent to solution) was determined. Thus, at a fixed initial solute concentration, an increase in the amount of sorbent offers a greater surface area.

3.2.3. Effect of pH

The removal of a CR from an aqueous solution is pH dependent due to the surface charge of the sorbent and the degree of the ionization of the dye. The influence of the pH in the range of 4–10, on the sorption of CR onto the 0.1 g L^{-1} of MIL-100(Fe) was investigated at constant initial concentration of 80 mg L^{-1} of CR, agitation speed of 250 rpm and at 30˚C (Fig. 7). As it can be seen in Fig. 7, as the pH value increases up to the pH of 6, the dye removal capacity is promoted and the maximum dye removal takes place at pH of 6–8. The two major sorption mechanisms for CR removal can be chemisorption and physical adsorption mechanisms. At the acidic pH, a considerably high electrostatic interaction occurs between the positively charged surface of the sorbent and the anionic dye. However, as the pH of the system increases, the number of negatively charged sites on the sorbent increases which does not favor the adsorption of the anionic dye due to the electrostatic repulsion. Thus, sorption of CR at alkaline pH is due to the chemisorption of CR on to the Fe open site of MIL-100 (Fe).

3.2.4. Kinetics of sorption

In order to explore the dynamics of the sorption procedure from the aqueous solution and to determine the potential rate-controlling steps, some kinetic models such as pseudo-first-order, pseudo-second-order, Elovich and intraparticle diffusion equation were applied to the experimental data at a pH of ~6.

Pseudo-first-order equation is based on the concept that the quantity of the change of the solute uptake with time is openly associated with the difference in saturation concentration and the amount of dye solid uptake with time. A simple pseudo-first-order equation is given by Lagergren equation [50]:

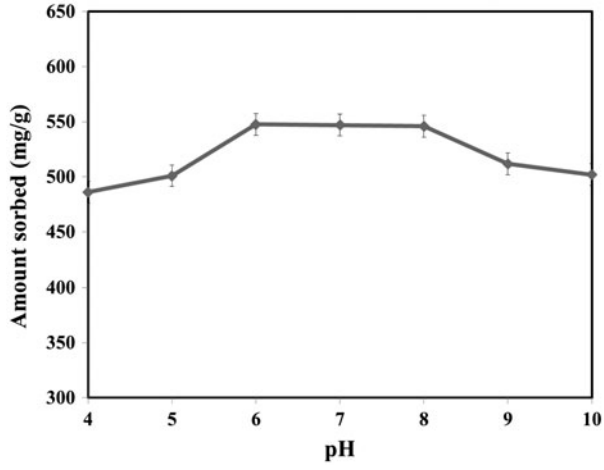

Fig. 7. Effect of pH on sorption of CR by MIL-100(Fe), (initial CR concentration = 80 mg L^{-1}, agitation speed = 250 rpm, sorbent dosage = 0.1 g L^{-1}, temperature = 30˚C).

$$\log(q_e - q_t) = \log q_e - \frac{k_1 t}{2.303} \quad (4)$$

where q_e and q_t are the amounts of the dye adsorbed (mg g^{-1}) at equilibrium time and any time t, respectively, and k_1 is the rate constant of sorption (min^{-1}). The rate constant, calculated q_e, and the corresponding linear regression correlation coefficient values obtained from the straight line plots of log (q_e–q_t) against t are given in Table 1.

The pseudo-second-order model is based on the assumption of chemisorption of the dye on the sorbent [51]. The pseudo-second-order equation is expressed as [51]:

$$\frac{t}{q_t} = \frac{1}{k^2 q_e^2} + \frac{t}{q_e} \quad (5)$$

where k_2 is the pseudo-second-order rate constant (g mg^{-1} min), q_e and q_t represent the amount of the dye adsorbed (mg g^{-1}) at equilibrium and at any time. The equilibrium sorption capacity (q_e), and the second order rate constant (k_2) are determined experimentally from the slope and intercept of the plot of t/q_t vs. t. The calculated constants (q_e, k_2), and the corresponding linear regression correlation coefficient values are provided in Table 1.

The Elovich equation widely used in adsorption kinetics describes the chemical adsorption mechanism in nature and is given by the following equation [52]:

$$q_t = \frac{1}{\beta}\ln(\alpha\beta) + \frac{1}{\beta}\ln t \quad (6)$$

where α is the initial sorption rate constant (mg g^{-1} min) and β is a factor associated with the degree of surface coverage and activation energy for chemisorption (g mg^{-1}). The values of α and β were calculated from the plot of q_t against ln t and the constants are also reported in Table 1.

When the dye adsorption is governed by the intraparticle mass transport rate, the diffusion (internal surface and pore diffusion) of the dye molecules inside the adsorbent, the rate-limiting step, can be presented by the following equation [52]:

$$q_t = K_{id}\, t^{\frac{1}{2}} + I \quad (7)$$

where I is the intercept and K_{id} is the intraparticle diffusion rate constant (mg g^{-1} min$^{1/2}$). According to this model, plot of q_t vs. $t^{1/2}$ should be linear if intraparticle diffusion is involved in the sorption process. Values of I give data about the width of the boundary layer. The calculated constants are also given in Table 1.

As realized from Table 1 and Fig. 8, the calculated linear regression correlation coefficient (R^2) of Elovich model (0.9969) and its small value of the Chi-square (0.4) suggested that the sorption of dye on the MIL-100(Fe) follows Elovich kinetics. Moreover, it has clearly been shown that among the three other models, the pseudo-second-order model with the good linearization ($R^2 = 0.9953$) describes the kinetics of CR sorption on MIL-100(Fe) in a better way. These results further support the assumption that the sorption is due to chemisorption. Similar results were also reported previously [53].

3.2.5. Sorption isotherm

The mechanism of the dye intercalation with the sorbent surface can be explained by sorption isotherms. To investigate the interaction of CR molecules and sorbent surface, different sorption models including Freundlich, Temkin, and Langmuir were employed. The Freundlich isotherm defines heterogeneous structures and multilayer reversible sorption formations. The Freundlich model is given in the following equation:

$$\mathrm{Ln}\, q_e = \ln K_f + \left(\frac{1}{n}\right)\ln C_e \quad (8)$$

where K_f and n are the Freundlich constants related to the sorption capacity (mg g^{-1}) and intensity, respectively.

The Langmuir equation is based on the theory that the structure of sorbent is homogeneous and all the sorption sites are undistinguishable with the equivalent energy. The Langmuir equation is represented as follow:

$$\frac{C_e}{q_e} = \left(\frac{1}{q_m b}\right) + \left(\frac{1}{q_m}\right)C_e \quad (9)$$

where q_e (mg g^{-1}) is the amount of the dye adsorbed at equilibrium, C_e is the equilibrium concentration of the dye in solution (mg L^{-1}), q_m (mg g^{-1}) is the Langmuir constant demonstrating maximum monolayer capacity, and b is the Langmuir constant associated with the sorption energy.

Temkin model assumes that the heat of the sorption of all the molecules in the layer decreases linearly

Table 1
Pseudo-first-order, pseudo-second-order, Elovich and intraparticle diffusion model constants for the removal of CR by MIL-100(Fe). ([CR] = 100 mg L^{-1}, agitation speed = 250 (rpm), sorbent dosage = 0.2 g L^{-1}, temperature = 30 ℃, pH 6)

Pseudo-first-order model					Pseudo-second-order model				Elovich model				Intraparticle diffusion model			
q_e (exp)	q_e (cal)	k_1	R^2	χ^2	q_e (cal)	k_2	R^2	χ^2	α	β	R^2	χ^2	k_{id}	I	R^2	χ^2
398.79	316.88	0.0104	0.9484	223.3	434.78	4.69×10^{-5}	0.9953	3.7	0.0036	0.0119	0.9969	0.4	14.07	135.2	0.9545	5.8

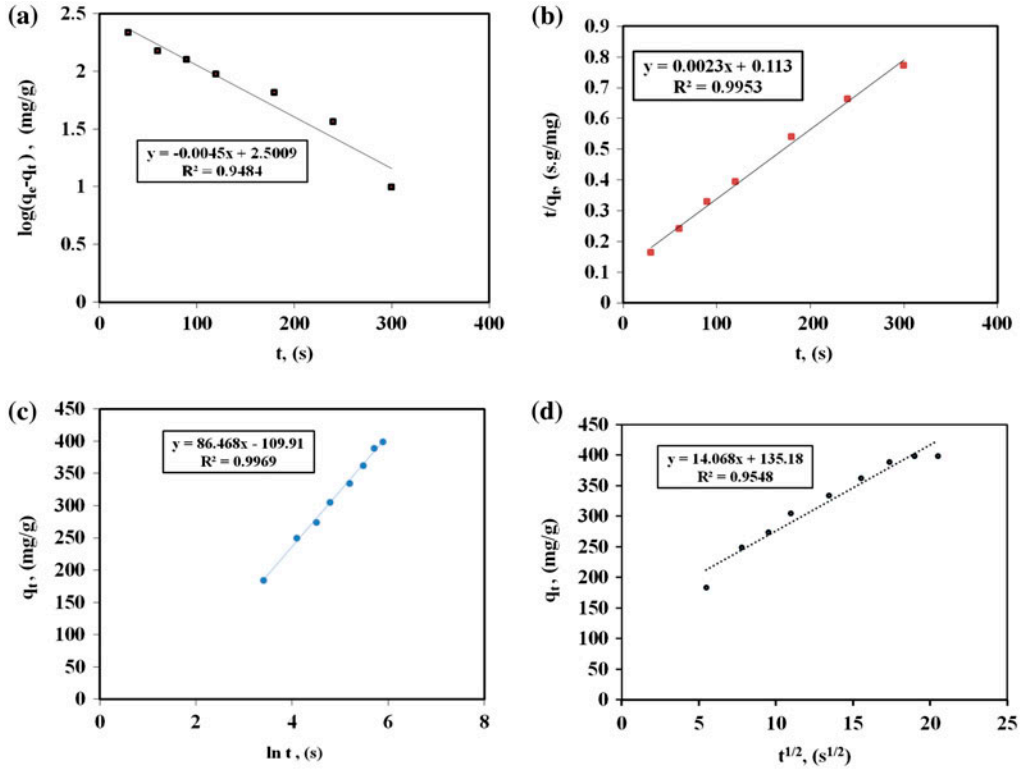

Fig. 8. (a) Pseudo-first-order, (b) pseudo-second-order, (c) Elovich, and (d) intraparticle diffusion isotherms for adsorption kinetics of CR by MIL-100(Fe), (agitation speed = 250 rpm, sorbent dosage = 0.2 g L^{-1}, initial dye concentration = 100 mg L^{-1}, temperature = 30 ℃, pH 6).

with the surface coverage due to the sorbent–dye interactions, and that the sorption is characterized by a uniform distribution of binding energies up to some maximum [54]. The Temkin isotherm is given as:

$$q_e = A \ln K_T + A \ln C_e \tag{10}$$

$$A = \frac{RT}{b} \tag{11}$$

K_T is the equilibrium binding constant (mol^{-1}) corresponding to the maximum binding energy and the constant A is related to the heat of the sorption.

The regression (R^2) and chi-square (χ^2) coefficients of the linearized isotherm data of the tree models at 25℃ and pH of ~6 are given in Fig. 9 and Table 2. The higher value of the correlation and the lower value of the χ^2 coefficients indicate a good agreement between the parameters and the best fitting of the Langmuir model to the experimental results. The q_m value for the sorption of CR by MIL-100(Fe) was 714.3 mg g^{-1} which shows the high mono layer sorption capacity of the iron based MOF sorbent.

3.2.6. Thermodynamic study of the sorption of dye on MIL-100(Fe)

Thermodynamic study of CR sorption onto the MIL-100(Fe) was done in the temperature range of 303–323 K with 200 mg L^{-1} CR and 0.3 g L^{-1} of sorbent. By increasing the temperature from 303 to 323 K the CR removal was increased from 597.85 to 613.17 mg g^{-1}) (Table 3).

The thermodynamic parameters including the Gibbs free energy (ΔG°), the enthalpy (ΔH°), and the entropy (ΔS°) were determined by the following equations:

$$K_c = Q_e / C_e \tag{12}$$

$$\Delta G^\circ = -RT \ln K_C \tag{13}$$

$$\ln K_C = \frac{\Delta S^\circ}{R} - \frac{\Delta H^\circ}{RT} \tag{14}$$

where K_C is the equilibrium constant, Q_e is the amount of the dye adsorbed per unit mass of the sorbent (mg g^{-1}), C_e is the equilibrium concentration (mg L^{-1})

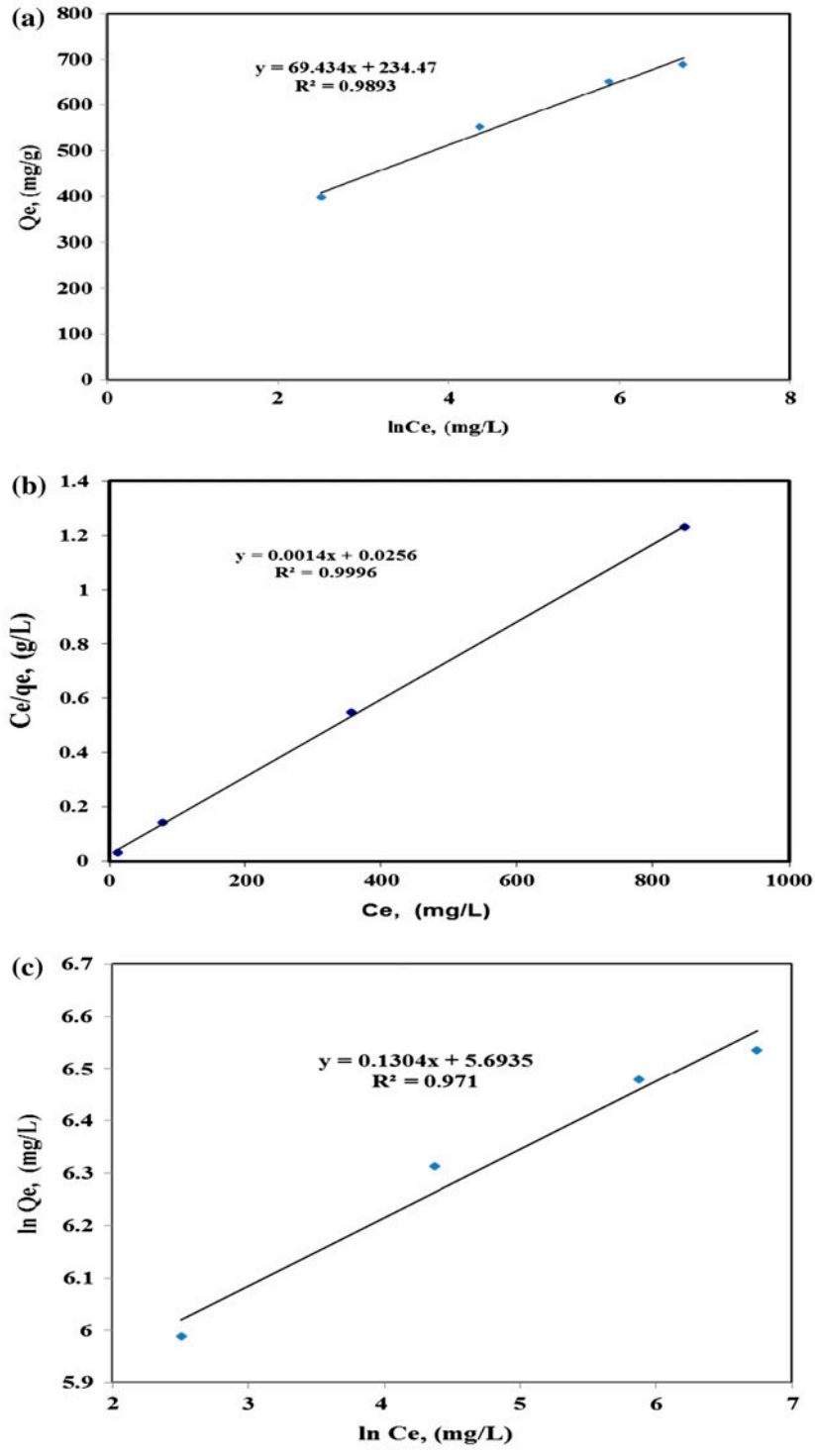

Fig. 9. (a) Langmuir, (b) Freundlich and (c) Temkin isotherms for adsorption of CR by MIL-100(Fe), (agitation speed = 250 rpm, sorbent dosage = 0.2 g L^{-1}, temperature = 30 ℃, pH 6).

of the dye solution, T (K) is the temperature, and R is the gas constant. The calculated thermodynamic parameters are also given in Table 3. K_c shows the ability of MIL-100(Fe) sorbent to retain CR and the extent of its movement in a solution phase [53] increased with an increase in the temperature from

Table 2
Temkin, Langmuir, and Freundlich constants for sorption of CR on MIL-100(Fe)

Langmuir				Freundlich				Temkin			
q_m (mg g^{-1})	b (L mg^{-1})	R^2	χ^2	K_F (mg g^{-1})	n (L mg^{-1})	R^2	χ^2	K_T	A	R^2	χ^2
714.3	0.0256	0.9996	2.8	296.93	7.67	0.971	3.0	1.34	234.47	0.9893	3.9

Table 3
Thermodynamic parameters for sorption of CR on MIL-100(Fe) ([CR] = 200 mg L^{-1}, agitation speed = 250 (rpm), sorbent dosage = 0.3 g L^{-1}, temperature = 303–323 K, pH 6)

T (K)	C_e (mg L^{-1})	q_e (mg g^{-1})	Kc	ΔG° (kJ mol^{-1})	ΔH° (kJ mol^{-1})	ΔS° (J mol^{-1} K)
303	20.64	597.85	28.95	−8.479	11.294	65.315
313	17.79	607.37	34.14	−9.188		
323	16.05	613.17	38.20	−9.782		

Table 4
The q_m values for the sorption of CR on different sorbents

Sorbent	q_m (mg g^{-1})	Reference
MIL-100 (Fe)	714.3	This work
CTAB-MMT	358	[55]
Chitosan/CNT	450.4	[56]
Cellulose/Fe_3O_4/activated carbon composite	66.09	[57]
Chitosan/montmorillonite nanocomposite	54.5	[58]

303 to 323 K. The negative values of ΔG° at different temperatures indicate the spontaneity of the sorption process. The positive ΔH° and ΔS° reveal that the sorption is endothermic and the disorder of the CR molecules is increased upon sorption, respectively.

4. Conclusions

Iron based MOF sorbent MIL-100(Fe) was synthesized and the structural order and the textural properties of the sorbent was studied by XRD, DTA/STA, FT-IR, and STM analyses and was used for the removal of CR from the aqueous solution.

Sorption kinetic of CR was found to confirm the Elovich and pseudo-second-order at a fixed MIL-100 (Fe) dosage. The sorption behavior could be described by Langmuir isotherm. Furthermore, the results indicate that the MIL-100(Fe) as an iron based MOF sorbent with high sorption capacity would be an excellent alternative to dye removal from the aqueous colored solutions. The monolayer sorption capacity of MIL-100(Fe) for the CR was found to be 714.3 mg g^{-1} which is much higher than the other sorbents used for the removal of the CR (Table 4) [54–58]. The superior sorption capacity of the MIL-100(Fe) may be attributed to its high BET surface area (2,800 m^2 g^{-1}) [46] and large specific pore volume (0.882 cm^3 g^{-1}) [46] as well as the presence of proper functional groups (open metal site and organic carboxylic acid group).

References

[1] K. Ravikumar, B. Deebika, K. Balu, Decolourization of aqueous dye solutions by a novel sorbent: Application of statistical designs and surface plots for the optimization and regression analysis, J. Hazard. Mater. 122 (2005) 75–83.
[2] H. Zollinger, Colour Chemistry: Synthesis Properties and Applications of Organic Dyes and Pigments, VCH Publishers, New York, NY, 1987.
[3] J.R. Easton, P. Cooper, Colour in Dyehouse Effluent, the Society of Dyers and Colorists, Alden, Oxford, 1995, pp. 9–21.
[4] P.K. Ray, Environmental pollution and cancer, J. Sci. Ind. Res. 45 (1986) 370–371.
[5] S. Chowdhury, P.D. Saha, Scale-up of a dye adsorption process using chemically modified rice husk: Optimization using response surface methodology, Desalin. Water Treat. 37 (2012) 331–336.
[6] G.S. Heiss, B. Gowan, E.R. Dabbs, Cloning of DNA from a Rhodococcus strain conferring the ability to decolorize sulfonated azo dyes, FEMS Microbiol. Lett. 99 (1992) 221–226.

[7] M.-C. Shih, Kinetics of the batch adsorption of methylene blue from aqueous solutions onto rice husk: Effect of acid-modified process and dye concentration, Desalin. Water Treat. 37 (2012) 200–214.
[8] R. Gong, Y. Ding, M. Li, C. Yang, H. Liu, Y. Sun, Utilization of powdered peanut hull as biosorbent for removal of anionic dyes from aqueous solution, Dyes Pigm. 64 (2005) 187–192.
[9] R. Han, D. Ding, Y. Xu, W. Zou, Y. Wang, Y. Li, L. Zou, Use of rice husk for adsorption of congo red from aqueous solution in column mode, Bioresour. Technol. 99 (2008) 2938–2946.
[10] S. Chatterjee, S. Chatterjee, B.P. Chatterjee, A.K. Guha, Adsorptive removal of congo red, a carcinogenic textile dye by chitosan, hydrobeads: Binding mechanism, equilibrium and kinetics, Colloid Surf. A: Physicochem. 299 (2007) 146–152.
[11] A. Mittal, V. Thakur, J. Mittal, H. Vardhan, Process development for the removal of hazardous anionic azo dye congo red from wastewater by using hen feather as potential adsorbent, Desalin. Water Treat. 52 (2014) 227–237.
[12] I.D. Mall, V.C. Srivastava, N.K. Agarwal, I.M. Mishra, Removal of congo red from aqueous solution by bagasse fly ash and activated carbon: Kinetic study and equilibrium isotherm analyses, Chemosphere 61 (2005) 492–501.
[13] G. Sharma, M. Naushad, D. Pathania, A. Mittal, G.E. El-desoky, Modification of *Hibiscus cannabinus* fiber by graft copolymerization: Application for dye removal, Desalin. Water Treat. (in press). doi: 10.1080/19443994.2014.904822.
[14] J. Mittal, D. Jhare, H. Vardhan, A. Mittal, Utilization of bottom ash as a low-cost sorbent for the removal and recovery of a toxic halogen containing dye eosin yellow, Desalin. Water Treat. 52 (2014) 4508–4519. doi: 10.1080/19443994.2013.803265.
[15] J. Mittal, V. Thakur, A. Mittal, Batch removal of hazardous azo dye bismark brown R using waste material hen feather, Ecol. Eng. 60 (2013) 249–253.
[16] A. Mittal, V. Thakur, V. Gajbe, Adsorptive removal of toxic azo dye amido black 10B by hen feather, Environ. Sci. Pollut. Res. 20 (2013) 260–269.
[17] A. Mittal, Removal of the dye, amaranth from waste water using hen feathers as potential adsorbent, Electron. J. Environ. Agric. Food Chem. 5 (2006) 1296–1305.
[18] A. Mittal, L. Kurup, Column operations for the removal and recovery of a hazardous dye 'acid red-27' from aqueous solutions, using waste materials—Bottom ash and de-oiled soya, Eco. Environ. Cons. 12 (2006) 181–186.
[19] A. Mittal, R. Jain, J. Mittal, M. Shrivastava, Adsorptive removal of hazardous dye quinoline yellow from waste water using coconut-husk as potential adsorbent, Fresenius Environ. Bull. 19 (2010) 1–9.
[20] A. Mittal, J. Mittal, L. Kurup, Utilization of hen feathers for the adsorption of indigo carmine from simulated effluents, J. Environ. Prot. Sci. 1 (2007) 92–100.
[21] A. Mittal, D. Jhare, J. Mittal, Adsorption of hazardous dye eosin yellow from aqueous solution onto waste material de-oiled soya: Isotherm, kinetics and bulk removal, J. Mol. Liq. 179 (2013) 133–140.
[22] M. Khadhraoui, H. Trabelsi, M. Ksibi, S. Bouguerra, B. Elleuch, Discoloration and detoxification of a congo red dye solution by means of ozone treatment for a possible water reuse, J. Hazard. Mater. 161 (2009) 974–981.
[23] P. Gharbani, S.M. Tabatabaii, A. Mehrizad, Removal of congo red from textile wastewater by ozonation, Int. J. Environ. Sci. Technol. 5 (2008) 495–500.
[24] K.P. Gopinath, S. Murugesan, J. Abraham, K. Muthukumar, *Bacillus* sp. Mutant for improved biodegradation of congo red: Random mutagenesis approach, Bioresour. Technol. 100 (2009) 6295–6300.
[25] M. Belhachemi, F. Addoun, Adsorption of congo red onto activated carbons having different surface properties: Studies of kinetics and adsorption equilibrium, Desalin. Water Treat. 37 (2012) 122–129.
[26] S. Chatterjee, D.S. Lee, M.W. Lee, S.H. Woo, Enhanced adsorption of congo red from aqueous solutions by chitosan hydrogel beads impregnated with cetyl trimethyl ammonium bromide, Bioresour. Technol. 100 (2009) 2803–2809.
[27] S.H. Lin, R.S. Juang, Y.H. Wang, Adsorption of acid dye from water onto pristine and acid-activated clays in fixed beds, J. Hazard. Mater. B113 (2004) 197–202.
[28] M. Alaei, A.R. Mahjoub, A. Rashidi, Effect of WO_3 nanoparticles on congo red and rhodamine B photo degradation, Iran. J. Chem. Chem. Eng. 31 (2012) 23–29.
[29] Z. Hasan, J. Jeon, S.H. Jhung, Adsorptive removal of naproxen and clofibric acid from water using metal-organic frameworks, J. Hazard. Mater. 209–210 (2012) 151–157.
[30] I. Ahmed, Z. Hasan, N. Khan, S.H. Jhung, Adsorptive denitrogenation of model fuels with porous metal-organic frameworks (MOFs): Effect of acidity and basicity of MOFs, Appl. Catal., B 129 (2013) 123–129.
[31] B.J. Zhu, X.Y. Yu, Y. Jia, F.M. Peng, B. Sun, M.Y. Zhang, T. Luo, J.H. Liu, X.J. Huang, Iron and 1,3,5-benzenetricarboxylic metal−organic coordination polymers prepared by solvothermal method and their application in efficient As(V) removal from aqueous solutions, J. Phys. Chem. C 116 (2012) 8601–8607.
[32] G. Ferey, C. Mellot-Draznieks, C. Serre, F. Millange, J. Dutour, S. Surble, I. Margiolaki, A chromium terephthalate-based solid with unusually large pore volumes and surface area, Science 309 (2005) 2040–2042.
[33] Y. Li, R.T. Yang, Gas adsorption and storage in metal organic framework MOF-177, Langmuir 23 (2007) 12937–12944.
[34] B. Chen, S. Ma, F. Zapata, F.R. Fronczek, E.B. Lobkovsky, H.C. Zhou, Rationally designed micropores within a metal-organic framework for selective sorption of gas molecules, Inorg. Chem. 46 (2007) 1233–1236.
[35] M. Eddaoudi, J. Kim, N. Rosi, D. Vodak, J. Wachter, M. O'Keeffe, O.M. Yaghi, Systematic design of pore size and functionality in isoreticular MOFs and their application in methane storage, Science 295 (2002) 469–472.
[36] H. Li, C.E. Davis, T.L. Groy, D.G. Kelley, O.M. Yaghi, Coordinatively unsaturated metal centers in the extended porous framework of $Zn_3(BDC)_3{\cdot}6CH_3OH$ (BDC) 1,4-benzenedicarboxylate), J. Am. Chem. Soc. 120 (1998) 2186–2187.

[37] J. Liu, P.K. Thallapally, B.P. McGrail, D.R. Brown, J. Liu, Progress in adsorption-based CO_2 capture by metal-organic frameworks, Chem. Soc. Rev. 41 (2012) 2308–2322.
[38] K. Sumida, D.L. Rogow, J.A. Mason, T.M. McDonald, E.D. Bloch, Z.R. Herm, T.H. Bae, J.R. Long, Carbon dioxide capture in metal-organic frameworks, Chem. Rev. 112 (2012) 724–781.
[39] H. Wu, Q. Gong, D.H. Olson, J. Li, Commensurate adsorption of hydrocarbons and alcohols in microporous metal organic frameworks, Chem. Rev. 112 (2012) 836–868.
[40] M.P. Suh, H.J. Park, T.K. Prasad, D.-W. Lim, Hydrogen storage in metal-organic frameworks, Chem. Rev. 112 (2012) 782–835.
[41] J. Rocha, L.D. Carlos, F.A.A. Paz, D. Ananias, Luminescent multifunctional lanthanides-based metal-organic frameworks, Chem. Soc. Rev. 40 (2011) 926–940.
[42] J.-R. Li, J. Sculley, H.-C. Zhou, Metal-organic frameworks for separations, Chem. Rev. 112 (2012) 869–932.
[43] C. Chen, M. Zhang, Q. Guan, W. Li, Kinetic and thermodynamic studies on the adsorption of xylenol orange onto MIL-101(Cr), Chem. Eng. J. 183 (2012) 60–67.
[44] E. Haque, J.W. Jun, S.H. Jhung, Adsorptive removal of methyl orange and methylene blue from aqueous solution with a metal-organic framework material, iron terephthalate (MOF-235), J. Hazard. Mater. 185 (2011) 507–511.
[45] E. Haque, J.E. Lee, I.T. Jang, Y.K. Hwang, J.S. Chang, J. Jegal, S.H. Jhung, Adsorptive removal of methyl orange from aqueous solution with metal-organic frameworks, porous chromium-benzenedicarboxylates, J. Hazard. Mater. 181 (2010) 535–542.
[46] R. Canioni, C. Roch-Marchal, F. Sécheresse, P. Horcajada, C. Serre, M. Hardi-Dan, G. Férey, J.-M. Grenèche, F. Lefebvre, J.-S. Chang, Y.-K. Hwang, O. Lebedev, S. Turner, G.V. Van Tendeloo, Stable polyoxometalate insertion within the mesoporous metal organic framework MIL-100(Fe), J. Mater. Chem. 21 (2011) 1226–1233.
[47] Y.K. Seo, J.W. Yoon, J.S. Lee, U. Lee, Y.K. Hwang, C.H. Jun, P. Horcajada, C. Serre, J.S. Chang, Large scale fluorine-free synthesis of hierarchically porous iron(III) trimesate MIL-100(Fe) with a zeolite MTN topology, Micropor. Mesopor. Mater. 157 (2012) 137–145.
[48] N.V. Maksimchuk, M.N. Timofeeva, M.S. Melgunov, A.N. Shmakov, Y.A. Chesalov, D.N. Dybtsev, V.P. Fedin, O.A. Kholdeeva, Heterogeneous selective oxidation catalysts based on coordination polymer MIL-101 and transition metal substituted polyoxometalates, J. Catal. 257 (2008) 315–323.
[49] M.T. Sulak, H.C. Yatmaz, Removal of textile dyes from aqueous solutions with eco-friendly biosorbent, Desalin. Water Treat. 37 (2012) 169–177.
[50] S. Lagergren, Zur theorie der sogenannten adsorption geloster Stoffe [For the theory of so-called adsorption of dissolved substances, The Royal Swedish Sciences]. Kungliga svenska vetenskapsakademiens, Handlingar Band. 24 (1898) 1–39.
[51] Y.S. Ho, G. McKay, Pseudo-second order model for sorption processes, Process Biochem. 34 (1999) 451–465.
[52] M. Özacar, I.A. Şengil, A kinetic study of metal complex dye sorption onto pine sawdust, Process Biochem. 40 (2005) 565–572.
[53] C. Namasivayam, D. Kavitha, Removal of congo red from water by adsorption onto activated carbon prepared from coir pith, an agricultural solid waste, Dyes Pigm. 54 (2002) 47–58.
[54] M.I. Temkin, V. Pyzhev, Kinetics of ammonia synthesis on promoted iron catalysts, Acta Physiochim. URSS 12 (1940) 327–356.
[55] L. Wang, A. Wang, Adsorption properties of congo red from aqueous solution onto surfactant-modified montmorillonite, J. Hazard. Mater. 160 (2008) 173–180.
[56] L. Wang, A. Wang, Adsorption characteristics of congo red onto the chitosan/montmorillonite nanocomposite, J. Hazard. Mater. 147 (2007) 979–985.
[57] H.-Y. Zhu, Y.-Q. Fu, R. Jiang, J.-H. Jiang, L. Xiao, G.-M. Zeng, S.-L. Zhao, Y. Wang, Adsorption removal of congo red onto magnetic cellulose/Fe_3O_4/activated carbon composite: Equilibrium, kinetic and thermodynamic studies, Chem. Eng. J. 173 (2011) 494–502.
[58] S. Chatterjee, M.W. Lee, S.H. Woo, Adsorption of congo red by chitosan hydrogel beads impregnated with carbon nanotubes, Bioresour. Technol. 101 (2010) 1800–1806.